

Supplementary Information:

Mechanistic study of hydrazine decomposition on Ir(111)

Xiuyuan Lu^a, Samantha Francis^a, Davide Motta^a, Nikolaos Dimitratos^{b*}, Alberto Roldan^{a*}

^a Cardiff Catalysis Institute, School of Chemistry, Cardiff University, Main Building, Park Place, Cardiff, CF10 3AT, UK

^b Department of Industrial Chemistry "Toso Montanari"; Alma Mater Studiorum-University of Bologna; Viale Risorgimento, Bologna, Italy

This file contains a compilation of figures and tables that complement the results and discussion in the publication with title “**Mechanistic study of the hydrazine decomposition on Ir(111)**”.

Content:

1. Surface structure of Ir(111) and Hydrazine
2. Surface energies and adsorption structures on IrO₂
3. Density of states (DOS) and projected density of state (PDOS) of hydrazine
4. Electron distribution of gas-phase and adsorbate hydrazine
5. Surface species on Ir(111)
6. Vibration modes of transition states
7. Vibration modes of ammonia and hydrazine
8. Reference

1. Surface structure of Ir(111) and Hydrazine

We have created a perfect Ir(111) surface, which is the most stable iridium surface exposing the close-packed plane of the fcc structure (**Fig. S1**). Iridium atoms at the surface model are arranged in a hexagonal lattice with a separation of 0.701 Å between nearest neighbour atoms, and there are four main adsorption positions: top, fcc site, hcp site and bridge.

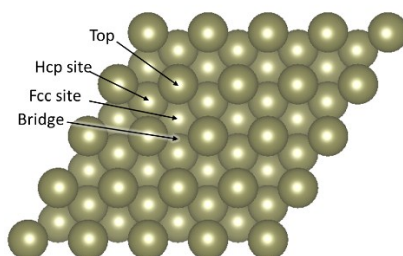


Fig. S1. The simulation perfect Ir(111) surface

Gauche is the most stable structure among the three dominant conformations of hydrazine (gauche, trans and eclipsed). As shown in **Fig. S2**, the optimized bond length of N-N and N-H in the hydrazine are 1.450 Å and 1.020 Å, respectively. The similar structure is used in many pieces of research.¹⁻⁴

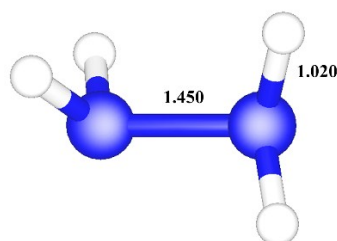


Fig. S2. The optimized structure of hydrazine

2. Surface energies and adsorption structures on IrO₂

The following data summarised the surface of the most common IrO₂ surfaces, **Table S1**, and the adsorption energies of the main species along the N₂H₄ decomposition, **Fig S3**.

Table S1. Surface energies of the most stable IrO₂ terminations and adsorption energies of the main species on these surfaces

	IrO ₂ (101)	IrO ₂ (110)	IrO ₂ (100)	IrO ₂ (001)	IrO ₂ (111)
γ_{hkl} (J/m ²)	1.46	1.82	2.34	2.74	2.83
N ₂ H ₄	-2.35	-3.24	-2.81	-	-
NH ₃	-2.02	-2.46	-2.69	-	-
N	-3.16	-3.65	-3.92	-	-
H	-3.13	-3.57	-3.46	-	-

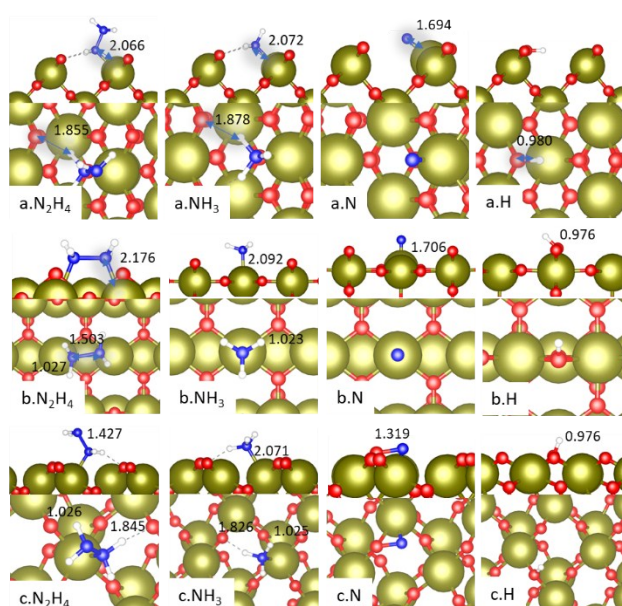


Fig. S3. Schematic representation of the most stable geometries of (from left to right) N₂H₄, NH₃, N and H.

3. Density of states (DOS) and projected density of state (PDOS) of hydrazine

The density of states (DOS) is defined by the equation:

$$DOS(E)dE = \text{number of levels between } E \text{ and } E + dE$$

The band structure of the surface determines the DOS curve's shape. Notably, the integral of DOS up to the Fermi level is the total *number* of occupied molecule orbitals. When the system is a close shell, this number times by two is the number of valence electrons. Hence, the DOS patterns also plot the distribution of electrons as a function of energy.⁵

The decomposition of the gauche N₂H₄ DOS is shown in **Fig. S4**, which can help us to trace down the bonding in the chemisorbed N₂H₄ system. It can be seen that 2p orbital of nitrogen

and 1s orbital of hydrogen form the bonding orbital π_1 and π_2 , while the antibonding orbital π^* was mainly contributed by the 2p orbital of nitrogen atoms. When the antibonding orbital π^* was been partly filled, the overlap of nitrogen 2p orbitals decreased, and π bond between the nitrogen was weakened.

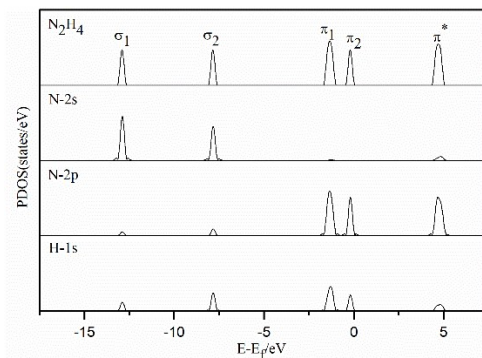


Fig. S4. Projected density of states of the orbital of N and H in the hydrazine

4. Electron distribution of gas-phase and adsorbate hydrazine

The Bader charge analysis is employed to characterize the electron distribution of gas-phase and adsorbate hydrazine. **Table S2** shows the details of the total valence electron in gas and adsorbed hydrazine. It suggests that 0.6 electrons transfer from hydrazine molecule to the surface, which is mainly contributed by the hydrogen in the molecule.

Table S2. The number of electrons in the gas phase and adsorbate N_2H_4

Atom	Gas-phase N_2H_4	Adsorbate N_2H_4
N1	5.81	5.76
N2	5.79	5.78
H1	0.59	0.47
H2	0.60	0.44
H3	0.59	0.47
H4	0.59	0.45
sum	13.97	13.37

5. Surface species on Ir(111)

Once N_2H_4 is adsorbed, we explored the adsorption sites and geometry of the different intermediates.

N_2H_3 . The N_2H_3 intermediate is a product of N_2H_4 dehydrogenation. This species prefers to sit on fcc hollow site with an adsorption energy of -2.97 eV. It lies with the NH part bridging

two surface atoms, i.e. η (2), with an Ir–N bond length of 2.104 Å. The NH₂ part has an Ir–N bond length of 2.125 Å and N–N bond elongate to 1.448 Å. These results are similar to those on Rh(111) and Cu(111) surfaces.^{6,7}

N₂H₂ has two isomers depending on the reaction pathway: HNNH and NNH₂. The binding of the HNNH structure on Ir(111) occurs through both nitrogen atoms positioned on hcp sites almost parallel to the surface and releases 2.47 eV. The NNH₂ intermediate adsorbs perpendicularly to the surface through a single N on an fcc hollow site ($E_{\text{ads}} = -2.79$ eV). The adsorption and molecular geometries are related to the N orbitals, which are also characterized by the N–N bond lengths, 1.341 and 1.372 Å for NNH₂ and HNNH respectively. These distances compare very well with previous benchmarks, i.e. 1.345 and 1.359 Å on Cu(111), and 1.429 and 1.367 Å on Rh(111) surface.^{6,7}

N₂H. Further dehydrogenation leads to N₂H intermediate, which preferentially adsorbs on a bridge site. This intermediate is firmly bound to the surface, $E_{\text{ads}} = -3.06$ eV, and the distance between the two nitrogen atoms is much shorter than in previous cases, 1.246 Å, showing an increment to the bond order although N–N is still longer than the same species in the gas phase (1.150 Å).⁸

N₂. The adsorption of molecular nitrogen was studied at different sites on the Ir(111) surface. The most stable configuration is N₂ parallel to the surface on a bridge site at 2.134 Å. The adsorption process releases 1.14 eV relative to gas-phase N₂. Moreover, the length of the N–N bond increased to 1.171 Å from 1.098 Å in the gas phase, which compares well with a reported experimental value of 1.098 Å.⁹

N adatoms adsorb preferably on fcc hollow sites releasing the energy of 0.56 eV relative to gas-phase N₂. The average distance between the three Ir atoms and N is 2.005 Å.

NH₃ prefers to adsorb on the top sites at 2.130 Å from neighboring Ir atoms. Exothermic adsorption of 1.95 eV (compared to isolated NH₃) results from the interaction of the NH₃ lone pair electrons with Ir 3d electrons.

NH₂. The bridge site is the most stable adsorption mode for NH₂, releasing 3.72 eV; this is larger than the other intermediates containing two nitrogen atoms (e.g. NNH₂, HNNH). The average Ir–N bond length is 2.104 Å. The N–H bond length (1.022 Å) is close to the experimentally reported distance in the gas-phase (1.024 Å).¹⁰

NH. The most stable adsorption site of imide is the hollow fcc ($\eta = 3$) perpendicular to the surface. This intermediate is largely stabilized by the surface ($E_{\text{ads}} = -4.31$ eV) for which the Ir–N bond length is of 2.020 Å. It shows that the adsorption energy is negatively correlated with the distance between N atom and Ir atoms in the surface.

H₂. Hydrogen molecules prefer to be physisorbed perpendicularly to the surface, releasing 0.53 eV due to long-range interactions. The result is close to the former theoretical studies ($E_{\text{ads}} = -0.46$ eV).¹¹ The distance to the surface Ir atoms is 2.578 Å for the top site.

H adatoms prefer to adsorb on the fcc sites of the Ir(111) surface. H lies at a distance of 1.900 Å to Ir with an adsorption energy of 0.86 eV in comparison to isolated H₂ molecule. This results in a stronger adsorption compared with a previous study ($E_{\text{ads}} = -0.41$ eV) as we considered dispersion corrections.¹²

6. Vibration modes of transition states

We have obtained the vibrational modes of every imaginary frequency, i.e. along the reaction direction, and summarised them in **Table S3**. Nearly all imaginary vibrations of dehydrogenation are N-H stretching expect NNH^* , which is due to N-H bending, and for the N-N split pathway, which imaginary vibration is along N-N stretching.

Table S3. The imaginary frequency and vibrational mode of transition states in the decomposition of N_2H_4

Reaction	Imaginary frequency(cm^{-1})	Vibrational mode
$\text{N}_2\text{H}_4^* \leftrightarrow \text{N}_2\text{H}_3^* + \text{H}^*$	956.9	N-H stretching
$\text{N}_2\text{H}_3^* \leftrightarrow \text{NNH}_2^* + \text{H}^*$	482.8	N-H stretching
$\text{N}_2\text{H}_3^* \leftrightarrow \text{HNNH}^* + \text{H}^*$	1126.8	N-H stretching
$\text{HNNH}^* \leftrightarrow \text{NNH}^* + \text{H}^*$	1115.8	N-H stretching
$\text{NNH}_2^* \leftrightarrow \text{NNH}^* + \text{H}^*$	386.1	N-H stretching
$\text{NNH}^* \leftrightarrow \text{N}_2^* + \text{H}^*$	910.2	N-H bending
$\text{N}_2\text{H}_4^* \leftrightarrow 2\text{NH}_2^*$	154.3	N-N stretching
$\text{N}_2\text{H}_3^* \leftrightarrow \text{NH}_2^* + \text{NH}^*$	356.9	N -N stretching
$\text{NNH}_2^* \leftrightarrow \text{NH}_2^* + \text{N}^*$	398.7	N -N stretching
$\text{NHNH}^* \leftrightarrow 2\text{NH}^*$	549.7	N -N stretching
$\text{NNH}^* \leftrightarrow \text{NH}^* + \text{N}^*$	571.9	N -N stretching
$\text{N}_2\text{H}_4^* + \text{NH}_2^* \leftrightarrow \text{N}_2\text{H}_3^* + \text{NH}_3^*$	335.8	N-H stretching
$\text{N}_2\text{H}_3^* + \text{NH}_2^* \leftrightarrow \text{HNNH}^* + \text{NH}_3^*$	268.3	N-H stretching
$\text{HNNH}^* + \text{NH}_2^* \leftrightarrow \text{NNH}^* + \text{NH}_3^*$	322.9	N-H stretching
$\text{N}_2\text{H}_3^* + \text{NH}_2^* \leftrightarrow \text{NNH}_2^* + \text{NH}_3^*$	252.5	N-H stretching
$\text{NNH}_2^* + \text{NH}_2^* \leftrightarrow \text{NNH}^* + \text{NH}_3^*$	654.9	N-H stretching
$\text{NNH}^* + \text{NH}_2^* \leftrightarrow \text{N}_2^* + \text{NH}_3^*$	1291.0	N-H stretching
$\text{NH}_3^* \leftrightarrow \text{NH}_2^* + \text{H}^*$	1229.5	N-H stretching
$\text{NH}_2^* \leftrightarrow \text{NH}^* + \text{H}^*$	1274.3	N-H stretching
$\text{NH}^* \leftrightarrow \text{N}^* + \text{H}^*$	1154.5	N-H stretching
$2\text{NH}_2^* \leftrightarrow \text{NH}^* + \text{NH}_3^*$	124.1	N-H stretching
$\text{NH}^* + \text{NH}_2^* \leftrightarrow \text{N}^* + \text{NH}_3^*$	213.9	N-H stretching
$2\text{N}^* \leftrightarrow \text{N}_2^*$	568.3	N-N stretching
$2\text{H}^* \leftrightarrow \text{H}_2^*$	271.1	H-H stretching

7. Vibration modes of ammonia and hydrazine

Fig. S5 and **Fig. S6** show the twelve vibration modes of hydrazine and the six of ammonia.

Our calculation results are in line with experimental research.¹³⁻¹⁷

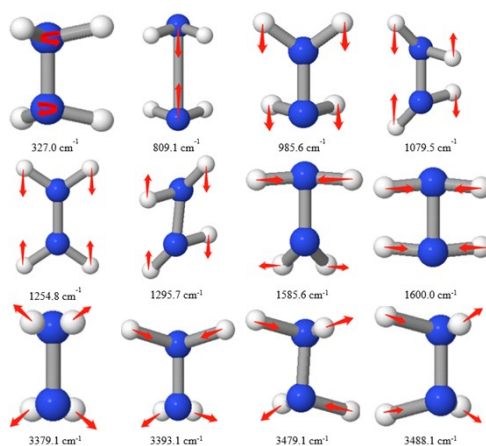


Fig. S5 Vibrational mode and frequency of the isolate hydrazine molecule

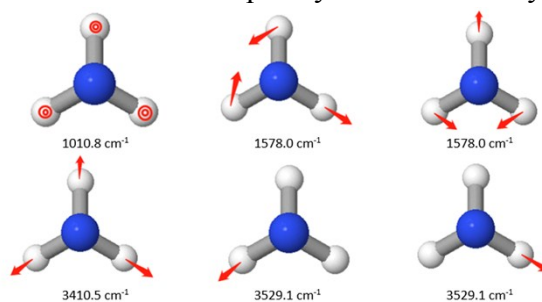


Fig. S6 Vibrational mode and frequency of the isolate ammonia molecule

Reference

1. Agusta, M. K.; Kasai, H., First principles investigations of hydrazine adsorption conformations on Ni(111) surface. *Surface Science* **2012**, *606* (7-8), 766-771.
2. Deng, Z.; Lu, X.; Wen, Z.; Wei, S.; Liu, Y.; Fu, D.; Zhao, L.; Guo, W., Mechanistic insight into the hydrazine decomposition on Rh(111): effect of reaction intermediate on catalytic activity. *Phys Chem Chem Phys* **2013**, *15* (38), 16172-82.
3. Tafreshi, S. S.; Roldan, A.; Dzade, N. Y.; de Leeuw, N. H., Adsorption of hydrazine on the perfect and defective copper (111) surface: a dispersion-corrected DFT study. *Surface Science* **2014**, *622*, 1-8.
4. Zhang, P.-X.; Wang, Y.-G.; Huang, Y.-Q.; Zhang, T.; Wu, G.-S.; Li, J., Density functional theory investigations on the catalytic mechanisms of hydrazine decompositions on Ir(111). *Catalysis Today* **2011**, *165* (1), 80-88.
5. Hoffmann, R., A chemical and theoretical way to look at bonding on surfaces. *Reviews of modern Physics* **1988**, *60* (3), 601.
6. Tafreshi, S. S.; Roldan, A.; de Leeuw, N. H. Density Functional Theory Calculations of the Hydrazine Decomposition Mechanism on the Planar and Stepped Cu(111) Surfaces. *Phys. Chem. Chem. Phys.* **2015**, *17* (33), 21533–21546. <https://doi.org/10.1039/C5CP03204K>.
7. Deng, Z.; Lu, X.; Wen, Z.; Wei, S.; Liu, Y.; Fu, D.; Zhao, L.; Guo, W. Mechanistic Insight into the Hydrazine Decomposition on Rh (111): Effect of Reaction Intermediate on Catalytic

- Activity. *Physical Chemistry Chemical Physics* **2013**, *15* (38), 16172–16182.
8. Pople, J. A.; Curtiss, L. A. The Energy of N₂H₂ and Related Compounds. *J. Chem. Phys.* **1991**, *95* (6), 4385–4388. <https://doi.org/10.1063/1.461762>.
 9. Huber, K. *Molecular Spectra and Molecular Structure: IV. Constants of Diatomic Molecules*; Springer US, 1979. <https://doi.org/10.1007/978-1-4757-0961-2>.
 10. Haynes, W. M. *CRC Handbook of Chemistry and Physics*; CRC Press, 2014.
 11. Ferrin, P. A.; Kandoi, S.; Zhang, J.; Adzic, R.; Mavrikakis, M. Molecular and Atomic Hydrogen Interactions with Au–Ir Near-Surface Alloys. *J. Phys. Chem. C* **2009**, *113* (4), 1411–1417. <https://doi.org/10.1021/jp804758y>.
 12. Liu, C.; Zhu, L.; Wen, X.; Yang, Y.; Li, Y.-W.; Jiao, H. Hydrogen Adsorption on Ir(111), Ir(100) and Ir(110)—Surface and Coverage Dependence. *Surface Science* **2020**, *692*, 121514. <https://doi.org/10.1016/j.susc.2019.121514>.
 13. Shimanouchi, T., Tables of molecular vibrational frequencies. Consolidated volume II. *Journal of physical and chemical reference data* **1977**, *6* (3), 993-1102.
 14. Koops, T.; Visser, T.; Smit, W., Measurement and interpretation of the absolute infrared intensities of NH₃ and ND₃. *Journal of Molecular Structure* **1983**, *96* (3-4), 203-218.
 15. Yamaguchi, A.; Ichishima, I.; Shimanouchi, T.; Mizushima, S.-I., Far infra-red spectrum of hydrazine. *Spectrochimica Acta* **1960**, *16* (11-12), 1471-1485.
 16. Durig, J.; Griffin, M.; Macnamee, R., Raman spectra of gases. XV: Hydrazine and hydrazine-d₄. *Journal of Raman Spectroscopy* **1975**, *3* (2-3), 133-141.
 17. Gurvich, L. V.; Veyts, I.; Alcock, C. B., *Thermodynamic Properties of Individual Substances: Elements O, H (D, T), F, Cl, Br, I, He, Ne, Ar, Kr, Xe, Rn, S, N, P and their compounds. pt. 1. Methods and computation. pt. 2. Tables*. Hemisphere: 1989; Vol. 1.